STRUCTURED PDMS USED AS ACTIVE ELEMENT FOR A BIOMIMETICS INSPIRED FLUID TRANSPORTER

Alexander Rockenbach and Uwe Schnakenberg

Institute of Materials in Electrical Engineering 1, RWTH Aachen University, Aachen, Germany

Abstract

A pneumatically actuated fluid transporter to transport fluids along surfaces is introduced. The biomimetic approach is based on the transportation principle of fluids by cilia or comb-row arrays due to the generation of metachronal waves. Rows of PDMS flaps which mimic comb-rows are asymmetrically positioned on flexible membranes. Each membrane is deflected by applying a defined pressure profile to achieve a metachronal wave on the surface. The simulations of the membrane behavior as well as a description of the concept by applying metachronal waves to the artificial comb row arrays are presented. The proof-of-concept shows fluid transport of up to 64 µm/s near the flap tips.

Keywords

PDMS, microfluidics, fluid transport, particle transport, biomimetics, cilia

Introduction

In microfluidic devices a couple of methods exist to transport particles in closed channels, e.g. pressure driven flow [1], electrophoresis [2], dielectrophoresis [3], or surface acoustic wave devices [4]. Particle or fluid transportation in open channels may be required in some cases. Here, the above described methods may fail due to the large distance or even absence of a cover plate.

In nature, many ciliated surfaces are known, e.g. in the respiratory tract or in the fallopian tube. Cilia are also used as propelling mechanism for microorganisms, e.g. Mesodinium rubrum, Paramecium, Volvox, Chlamydomonas reinhardtii, Ctenophore. These cilia arrays often move in a synchronized manner with a certain phase shift between adjoined cilia to optimize the transportation or self-propulsion. The biological actuation principle can vary over the different species.

In the biomimetic approach to mimic biological cilia, different techniques of forming artificial cilia and methods to stimulate those were introduced in the last decade, such as electrostatic forces [5, 6], magnetic field [7–11], light-excitation [12], chemical [13–15], or mechanical forces [16]. However, the fabrication processses of all these approaches suffer from high costs and complexity. On the other hand, soft-lithography and micro molding of polydimethyl-siloxane (PDMS) are established as techniques for the production of low-cost microfluidic devices. They can ideally be used for fabrication of flexible membranes and flaps.

The objective of this paper is the investigation of the propelling mechanism of a pneumatically working artificial comb row, which can be easily fabricated using standard low-cost soft-lithography and micromolding techniques. The concept is shown in Figure 1 and is already published in [17]. Rows of cilia-like flaps are positioned on bendable membranes out of the center of regularly separated cavities. Each flap row can be deflected separately by an induced pneumatic pressure from the back side into the cavity, which then leads to a bending of the supporting membrane. Due to the high aspect ratio of the flaps the membrane deflection results in a considerable large transversal motion of the flap tips. In addition, as a reaction to the pressure profile the outward motion may differ in the temporal profile from the inward motion of the membrane, an asymmetry in the temporal motion cycle between the forward and backwards directed stroke is imposed. The bending cycle between adjacent channels can be adjusted so that it replicates a metachronal wave.

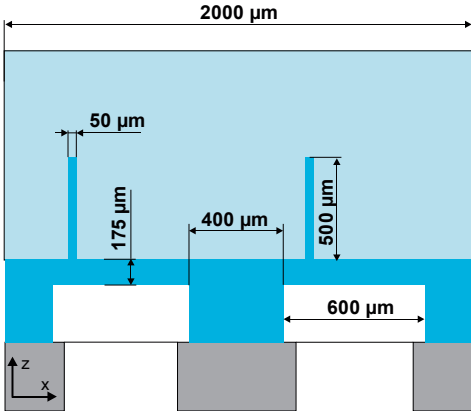

Fig. 1: Design details of the layout: the pressure channel (cavity) under the 175 µm thick membranes is 600 µm wide. In combination with the 400 µm wide supporting structure between two channels a pitch of 1000 µm is defined. The flaps are 500 µm high, 50 µm thick and 10000µm long, respectively.

Design Concept

Layout details of the membrane and the flap structure are shown in Figure 1. The width of the supporting structure was set to 400 µm and the width of the cavity to 600 µm, respectively. Typically, 500 µm high (h) and 50 µm wide flaps were used as artificial comb rows that extend into the fluid from the flexible surface wall. To move the fluid effectively and not only in the vicinity of the membrane the design must show some kind of asymmetry, therefore the flap is positioned out of center. This first asymmetry enables the flap to transport the fluid in the desired direction.

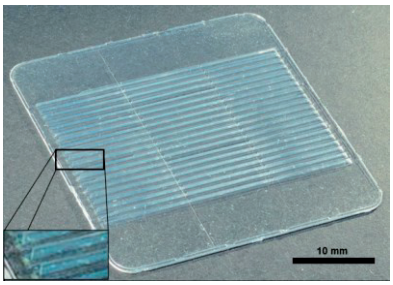

Fig. 2: Photograph of the artificial comb row array. 20 rows of flaps are located on flexible membranes (not shown while on the back side). Each channel is 30 mm long. On each membrane three 10 mm long flaps are located. The fabrication is published in [18].

A second asymmetry is induced by the asymmetric movement of the flap. By applying the metachronal wave, the movement of each flap is strongly coupled to its neighbors. This coupling enforces the stroke of the flap by changing the beat path. The membranes are stretched and compressed by the neighboring membranes. When a membrane is moving upwards the pressure in the cavities in front are pushing the flap forward. This increases the absolute height of the flap in the fluid during the effective stroke.

On the other hand, the contracted membranes behind the recovering membrane are pulling the flap back and down. The behavior is shown in Figure 3 which is composed of superposed pictures of a beating single flap. The colored track represents the path of one edge of the flap tip. The total height difference on the 342 µm long path is 85 µm which corresponds to 25% relative to the flap height.

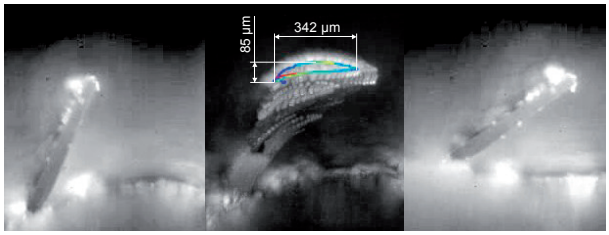

Fig. 3: Photos of flap movements to illustrate the asymmetry. Left: Negative pressure – start position. Middle: Superposed pictures of beating cycles of single flap tip where several particles are fixed. The colored circle corresponds to the tip movement of the flap. The picture shows the deflection hysteresis of the flap tip. Right: Positive pressure – maximum deflection.

Furthermore, a third type of asymmetry corresponds to the applied pressure profile under the membranes, which is also advantageous for the fluid transport: The pressure behavior depends on several parameters: magnitude and direction of the pressure change, fluid impedance and resistance of the connecting tubes between valve and connector. For illustration, Figure 4 shows the pressure profiles for four applied pressures measured in one cavity for a 500 mm long tube. The black curve refers to the valve position and reflects the switching behavior of the valve.

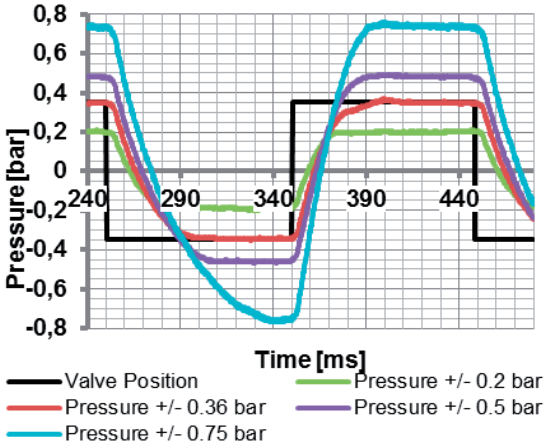

Fig. 4: Four applied pressures measured in one channel with respect to time. The black curve refers to the valve position and reflects the switching behavior of the valve (100 ms). The tube length between valve and connector was set to 500 mm.

After switching the valve from high to low pressure level the pressure in the cavity decreases until it reaches the lower level. A higher pressure difference corresponds to a longer decay time for reaching the lower level, e.g. a pressure step from +0.75 bar to −0.75 bar takes 90 ms, whereas a step from +0.2 bar to –0.2 bar takes only 30 ms. The opposite pressure change from low to high level is significantly faster. Here, a pressure change from –0.75 bar to +0.75 bar takes 45 ms, whereas a step from +0.2 bar to –0.2 bar takes only 20 ms.

The characteristic pressure delay behavior between the applied pressure and the pressure in the cavity under the membrane can be used for generating an asymmetric behavior of the flap movement. A fast positive pressure difference induces the energy faster into the system then the slower negative pressure difference does. Following the notation of biology, a positive switch (from low to high) defines the effective stroke of the flaps, whereas a negative switch (from high to low) represents the slow recovery stroke. This anisotropy is assumed to support the net transport in direction of the effective stroke. To create a travelling wave mechanism in the flap array pressures were switched from +0.6 bar to –0.6 bar to all of the twenty membranes consecutively, as demonstrated in a simulation model (Figure 5).

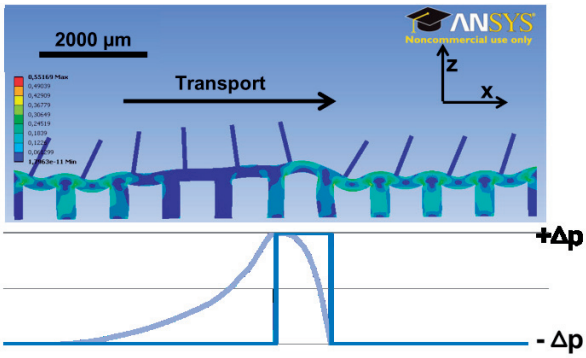

Fig. 5: Top: Travelling wave chronology. The metachronal wave is applied from right to left, as the flaps are numbered. Effective stroke (positive pressure) is applied between flap 5 and 6. From flap 3 to flap 5 the membrane deformation as well as the flap deflection corresponds to the application of the recovery stroke. Bottom: The light line shows the valve-pressure, whereas the dark line corresponds to the membrane pressure.

Simulations

Simulations were carried out using ANSYS 12 Structural program based on a 2D model with high deformation. The material data for PDMS (poly(dimethylsiloxane), Sylgard 184, Dow Corning, Midland, USA), which serves as suitable material for the membrane and flaps, was defined as an isotropic material model. The material parameters were generated by tensile testing [19]. Optimum membrane bending conditions were extracted for a 600 µm wide and 100 µm thick PDMS membrane. The supporting structure between two membranes was optimized to 400 µm. The van Mises stress distribution of the PDMS membrane is shown in Figure 6, when the membrane is deflected by a pressure of 40 kPa. With respect to the soft membrane material, the bending deforms the membrane shape and increases the membrane area. These deformations appear in both bending directions of the membrane and are responsible for a shift of the tip deflection.

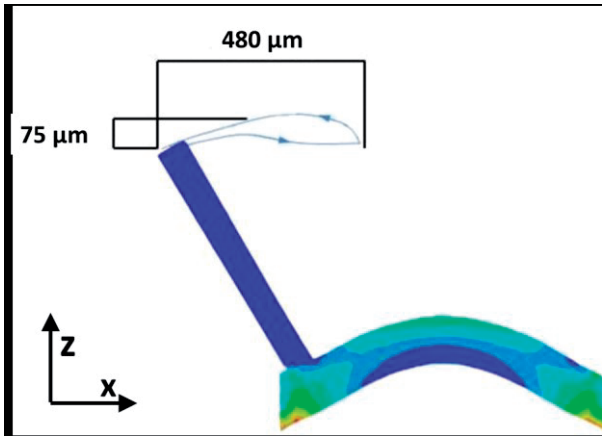

Fig. 6: ANSYS 12 FEM simulation of van Mises stress distribution of a 100 µm thick PDMS membrane deflected by a pressure of 40 kPa.

The asymmetric flap position on the membrane results in an asymmetrical movement of the flap. Figure 6 shows the simulated movement of the flap by setting a minimum and maximum pressure difference of 40 kPa and -30 kPa compared to ambient pressure. The flap moves 480 µm in x-direction and 75 µm in z-direction. This behavior generates a lateral movement in the fluid. A similar characteristic movement was published by Khaderi et al. [20].

Results

At first, the real flap movement were analyzed and compared to the simulation results. As mentioned before, the coupling of neighboring membranes enforces the stroke of the flap by increasing the absolute height of the flap in the fluid during the effective stroke. This behavior was simulated in Figure 6 and is verified in Figure 3 experimentally. Both, simulation and experiment showed the same difference in forward and backward stroke. In the simulation the tip movement of 480 µm in x-direction and 75 µm in z-direction was calculated. This is a relative difference of 16%.

This behavior is crucial to transport fluids in the regime of laminar flow, because in general a reversible

movement in a laminar flow regime cannot produce an effective transport of the fluid. In a rough estimation the Reynolds number Re can be calculated to:

$$Re = \frac{\rho v L}{\mu} \qquad (1)$$

where ρ is the density (1060 kg/m³), L the height of the fluid (6 mm) and μ the viscosity (0.001 Pa*s), respectively. The characteristic velocity v is hard to determine, but can be estimated to be between the maximum velocity of flap tip in the power stroke of 7600 µm/s and the total flow velocity of the fluid of 40 µm/s. Using this velocity range, Re varies from 0.25 to 48. Both values are in the range of laminar flow. This indicates the importance that only asymmetries in the stroke result in fluid transport, which is also known from natural cilia and comb-rows [21, 22].

To perform fluid transport in the system the transporter device was connected to a pneumatic triggering module and integrated into a microfluidic chamber. A glycol-water mixture of 3:10 was used as fluid to ensure levitating particles. Fluorescence-marked 60 µm polystyrene particles were used for experiments. Figure 7 shows a snap-shot of the proof-of-concept. Several particles are shown in the flap array. The different diameters correspond to the different vertical positions the particles have corresponding to the focus depth of the objective lens (focus is adjusted on top of the flap). The trajectories of some particles are shown. The particle transportation direction was from the left to the right. Depending on the relative position between particle and flap, a net transport velocity was determined to be 40 µm/s.

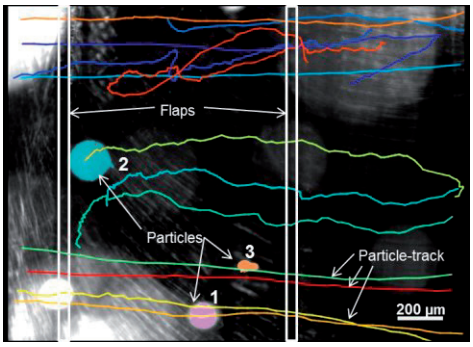

Fig. 7: Photograph (top view) of a detail of membrane and flap arrangement. The focus is set on the membrane surface. The membranes and the flaps were arranged vertically. Fluorescence-marked 60 µm polystyrene particles were shown. The different diameters refer to different distances of the particles from the membrane surface. Particles were transported by the travelling wave moving along the flap array. Wave velocity: 20 mm s^{-1}, duty cycle: 0.1, wave length: 20 mm. Selected particle paths are shown in color. The particles were transported from right to left with typical velocities of 40 µm/s. The gray shadows mainly observed in the lower left corner results from the rough surface of the connector.

Depending on the vertical distance of the particle from the membrane surface the particle velocity varies considerably. Particle tracks in vicinity to the flap tips at y ≈ h showed often straight lines (lilac particle, 1) with velocities up to 64 µm/s, whereas particles farther above the tip at y ≈ 2h showed less flow speed (light blue particle, 2) of 22 to 31 µm/s. This behavior indicates a rather homogenous fluid stream with high velocity next to the flap tips. The net transport velocity was determined from all tracks to approximately 40 µm/s. Similar fluid speeds were reported using discontinued flap arrays with a single flap length of 0.9 mm and a gap of 0.1 µm between two flaps [17]. In addition, the same order of flow speeds was calculated in numerical simulations of flow generated by the cilia on Ctenophores [23] using flaps of the same scale as in our experiments.

Conclusion

The active movement of comb row like flaps induces a fluid flow. The flaps are actuated through pneumatic pressure applied to the backside of a membrane. Simulations are carried out to optimize the design. The asymmetric position of the flaps on the membrane results in an asymmetric movement of the flaps. Mean velocities of 40 µm/s were obtained by applying metachronal waves to the flap array.

In future devices the transport efficiency must be optimized. The device dimensions must be significantly reduced to be able to integrate it in microsystems, e.g. for microfluidic applications.

Acknowledgement

Funding was given by the German Federal Ministry of Education and Research under grant #16SV5341 (PaTra).

References

[1] Squires TM, “Microfluidics : Fluid physics at the nanoliter scale,” Rev. Mod. Phys., vol. 77, no. July, pp. 977–1016, 2005.

[2] Wu D et al., “Electrophoretic separations on microfluidic chips.” J. Chromatogr. A, vol. 1184, no. 1–2, pp. 542–59, Mar. 2008.

[3] Markx GH and Davey CL, “The dielectric properties of biological cells at radiofrequencies: applications in biotechnology,” Enzyme Microb. Technol., vol. 25, no. 3–5, pp. 161–171, Aug. 1999.

[4] Friend J and Yeo LY, “Microscale acoustofluidics: Microfluidics driven via acoustics and ultrasonics,” Rev. Mod. Phys., vol. 83, no. 2, pp. 647–704, Jun. 2011.

[5] Osterman N and Vilfan A, “Finding the ciliary beating pattern with optimal efficiency.,” Proc. Natl. Acad. Sci. U. S. A., vol. 108, no. 38, pp. 15727–32, Sep. 2011.

[6] Alexeev A et al., “Designing synthetic, pumping cilia that switch the flow direction in microchannels,” Langmuir, vol. 24, no. 21, pp. 12102–12106, 2008.

[7] Vilfan M et al., “Self-assembled artificial cilia.,” Proc. Natl. Acad. Sci. U. S. A., vol. 107, no. 5, pp. 1844–7, Feb. 2010.
[8] Timonen JVI et al., “A facile template-free approach to magnetodriven, multifunctional artificial cilia.” ACS Appl. Mater. Interfaces, vol. 2, no. 8, pp. 2226–30, Aug. 2010.
[9] Gao Y et al., “Strong vortical flows generated by the collective motion of magnetic particle chains rotating in a fluid cell.” Lab Chip, Nov. 2014.
[10] den Toonder JMJ and Onck PR, “Microfluidic manipulation with artificial/bioinspired cilia.” Trends Biotechnol., vol. 31, no. 2, pp. 85–91, Feb. 2013.
[11] Khaderi SN et al., “Magnetically-actuated artificial cilia for microfluidic propulsion.” Lab Chip, vol. 11, no. 12, pp. 2002–10, Jun. 2011.
[12] van Oosten CL et al., “Printed artificial cilia from liquid-crystal network actuators modularly driven by light.” Nat. Mater., vol. 8, no. 8, pp. 677–682, Aug. 2009.
[13] Zarzar LD et al., “Bio-inspired design of submerged hydrogel-actuated polymer microstructures operating in response to pH.,” Adv. Mater., vol. 23, no. 12, pp. 1442–6, Mar. 2011.
[14] Sanchez T et al., “Cilia-like beating of active microtubule bundles.” Science, vol. 333, no. 6041, pp. 456–9, Jul. 2011.
[15] Dayal P et al., “Chemically-mediated communication in self-oscillating, biomimetic cilia,” J. Mater. Chem., vol. 22, no. 1, p. 241, 2012.
[16] Brücker C and Keissner A, “Streaming and mixing induced by a bundle of ciliary vibrating micro-pillars,” Exp. Fluids, vol. 49, no. 1, pp. 57–65, Nov. 2009.
[17] Rockenbach A et al., “Pneumatically Actuated Biomimetic Particle Transporter,” in 2014 IEEE 27th International Conference on Micro Electro Mechanical Systems (MEMS 2014), 2014, pp. 927–930.
[18] Rockenbach A et al., “Fluid transport via pneumatically actuated waves on a ciliated wall,” J. Micromechanics Microengineering, vol. 25, no. 12, p. 125009, 2015.
[19] Klammer I et al., “Numerical analysis and characterization of bionic valves for microfluidic PDMS-based systems,” J. Micromechanics Microengineering, vol. 17, no. 7, pp. S122–S127, Jul. 2007.
[20] Khaderi SN et al., “Magnetically-actuated artificial cilia for microfluidic propulsion.” Lab Chip, vol. 11, no. 12, pp. 2002–2010, Jun. 2011.
[21] Goldstein R et al., “Noise and Synchronization in Pairs of Beating Eukaryotic Flagella,” Phys. Rev. Lett., vol. 103, no. 16, p. 168103, Oct. 2009.
[22] Dauptain A et al., “Hydrodynamics of Beating Cilia,” Symp. A Q. J. Mod. Foreign Lit., pp. 1–10, 2007.
[23] Brennen C and Winet H, “Fluid Mechanics of Propulsion by Cilia and Flagella,” Annu. Rev. Fluid Mech., vol. 9, pp. 339–98, 1977.

Uwe Schnakenberg, Dr.-Ing.
Institute of Materials in Electrical Engineering 1
RWTH Aachen University
Sommerfeldstraße 24, 52074 Aachen, Germany

E-mail: schnakenberg@iwe1.rwth-aachen.de
Phone: +49 241 80 2784